Hamiltonian Analytical Optics and Simulations of Betatronic Motion by Optical Devices.

A. Bazzani*, P. Freguglia **, G. Gradoni***, G. Turchetti *

* *Dipartimento di Fisica e Astronomia,Universitá di Bologna and INFN Sezione di Bologna*
** *Dipartimento di Ingegneria e Scienze dell'Informazione, Universitá dell'Aquila*
*** *School of Mathematical Sciences and George Green Institute for Electromagnetic Research, University of Nottingham*

The aim of our contribution is to present the analogy between the Hamiltonian Analytical Optics and the Beam Dynamics. We follow the Hamilton's memoir by means of a revision of the text, where it is discussed an application of Lagrange δ-calculus. After an philological introduction we consider the correspondence between the trajectory of particles in a circular accelerator and rays in an optical system or a wave guide. An experiment, with a laser on an optical system with mirrors and lenses simulating a FODO cell, showed that the ray bundles move on an ellipse in agreement with the linear theory. We consider here a cylindrical optical fiber with a radially varying refraction index such that $n^2(r)$ is quadratic to reproduce the betatronic beam dynamics between two subsequent nonlinear equally spaced thin elements. The nonlinear effect can be introduced with short nonlinear insertions where n^2 depends on the transverse coordinates x, y and is polynomial of degree three or higher. The Poincaré map for the rays is approximated by the Hénon map, which describes the beam dynamics, provided that d the rays do not reach the boundary where the refections would introduce a different dynamic behavior. Indeed the billiard like dynamics of rays reflecting at boundaries has been analyzed in the literature for laser beams propagating in a waveguide or an optical cavity and the chaotic behaviour was found to be relevant for applications, but the correspondence with beam dynamics is lost.

Keywords: Analytic Optics, Beam Dynamics, Analogical Experiments, Nonlinear Effects.

1. Introduction

The laws which characterized the classical geometrical optics before W.R. Hamilton[1], laws which depend on the optical experience and researches, are the following results (as postulates or axioms) :

- A.1: The rays of light propagate as straight lines.
- A.2: The angles of incidence and of reflection (which stay in the same plane) are equal.
- A.3: Relating to the refraction, the rays obey the sinus law.
- A.4: The light rays cross without thwarting themselves.
- A.5: The light velocity is finite and constant.

Extending the validity of these Principles, he established a fundamental analogy between Optics and Mechanics. In fact Hamilton bases his method on a combination

of a Variational Principles with partial differentials equations and the individualization of a *characteristic function* in optics (which depends on the fundamental laws of the catoptrics) together with a *principal function* in mechanics (which depends on Newton's equations). In the history of Mechanics this analogy was considered at least for another important occasion: the solution of the brachistochrone problem by Johann Bernoulli in a memoir of 1697[2]. It is the following well known problem: given two points A and B in a vertical plane to find the path AMB down which a movable point M must, by virtue of its weight, proceed from A to B in the shortest possible. time. Johann ibid writes:

> [...] Leibniz, in the Acta Eruditorum, 1682, pp. 185 and successively, and soon the famous Huygens in his Treatise on light, p.40, have demonstrated this more comprehensively and, by most valid arguments, have established the physical, or better the metaphysical principle which Fermat seems to have abandoned [...], remaining satisfied with his geometric proof and giving up the rights all too lightly.

Johann reverses the arguments, so

> Now we shall consider a medium that is not homogeneously dense, but consists of purely parallel horizontally superimposed layers, each of which consists of a diaphanous matter of a certain density decreasing or increasing according to a certai law. It is then manifest that a ray which we consider as a partcle will not be propagated in a straight line, but in a curved path [...].

By means of this analogy Johann Bernoulli resolves in a neat way the brachistocrone problem[a]

The topic of the analogy Optics-Mechanics is also linked to so-called Fermat's principle of least time and to the least action principle of Maupertuis. Of cours even the recherches of Leibiniz and of Newton have to seen and analyzed[b].

Beam Dynamics of large colliders has opened a new field of application to Classical Mechanics, due to the presence of nonlinear effects introduced by multipolar magnets. Understanding the role of nonlinear resonances which overlap creating regions of chaotic motion in phase, which induce particles transport, is a key issue to provide an analytical stability estimates and to control the boundary of rapid escape region (dynamic aperture)[5]. The validation of the proposed models and methods, such as the Birkhoff normal forms[5], requires an experimental activity on the accelerator machine that can be both expensive and complex due to the setup requirements. From this viewpoint the possibility of proposing optical experiments based on the analogy between Geometrical Optics and Classical Mechanics can be helpful for the study of some nonlinear effects and for an analogic simulation of beam dynamics[6]. In this paper we extend a previous proposal based on an optical system with lenses and mirrors, where the nonlinear effects are introduced by aberrations[7], by considering the nonlinear dynamics of a laser beam propagating in an optical fiber with a varying refraction index. The propagation of light in fibers and cavities has been intensively investigated and the onset of chaotic behavior

[a]See[3] pp. 39-45

[b]See[4] Chap.V, pp.255-275. This book includes a lot of historical topics about the mechanics.

has been exploted to concentrate and extract the light. The optical simulation we consider consists of a cylindrical fiber with a radially decreasing refraction index to focus the light on the axis and short insertions to simulate the non linear effect of a sextupole or higher multipole. In this way a correpondence with the dynamics of a FODO cell, the basic unit of a symmetric ring, is obtained. The conditions to insure the paraxial approximation, to avoid the reflection on the fiber boundary and to prevent reaching the fast instability region, delimited by the dynamic aperture, are examined. These conditions are fulfilled for the typical parameters range of a symmetric circular accelerator. Arranging the fiber of a few mm radius as a circular ring 3 m long the light makes one million turns in 10 ms and the major issues are the injection and the turn by turn detection of the phase space coordinates of a single ray or of a rays bundle, described by the Liouville equation. Though the correspondence with the beam dynamics is lost, the optical fibers or cavities, where reflection take place, are very interesting from the point of of dynamics and for for applications. A short review of the subject is presented.
The possibility of simulating the run of a hadron accelerator with a small apparatus is appealing and if the injection and detection problems can be solved it might be complementary to numerical simulations.

1.1. *Algebraic expressions of the reflection and the refraction*

At first we consider the reflection case [c]. Hamilton says:

> "[1.] When a ray of light is reflected at a mirror, we know by experience, that the normal to the mirror, at the point of incidence, bisects the angle between the incident and the reflected rays. If therefore two forces, each equal to unity, were to act at the point of incidence, in the directions of the two rays, their resultant would act in the direction of the normal, and would be equal to twice the cosine of the angle of incidence".

ρ denotes the incident ray and ρ' the reflected ray. Now, if we denote by ρl, $\rho' l$, nl, the angles which the two rays and the *normal* make respectively with any assumed line l and by I the angle of incidence, we shall have the following formula:

$$\cos \rho l + \cos \rho' l = 2 \cos I \cos nl \tag{1}$$

which is the analytic representation of the known law of reflection.

Of course $\rho = \rho(x, y, z)$ and $\rho' = \rho'(x, y, z)$. If we denote by: ρx, ρy, ρz; $\rho' x$, $\rho' y$, $\rho' z$; nx, ny, nz the angles which the two rays and the normal make respectively with three rectangular axes, x, y, z, from (1), we obtain the equations:

[c]See W.R.Hamilton, "Theory of systems of rays" (1828). Part First *On ordinary system of reflected rays,* Section I. *Analyrtic expression of the law of ordinary reflection*

$$\begin{cases} \cos\rho x + \cos\rho' x = 2\cos I\cos nx \\ \cos\rho y + \cos\rho' y = 2\cos I\cos ny \\ \cos\rho z + \cos\rho' z = 2\cos I\cos nz \end{cases} \tag{2}$$

which determine the direction of the reflected ray, when we know that one of incident ray, and the tangent plane to the mirror[d].

Likewise for the refraction Hamilton[e] determines the following formula

$$\cos\rho l + m\cos\rho' l = (\cos\rho n + m\cos\rho' n)\cos nl \tag{3}$$

where: $m = \frac{\sin\rho n}{\sin\rho' n}$, m depends on the nature of the mediums, ρ is the incident ray, ρ' is the refracted ray and n is the normal. ρn and $\rho' n$ are the angles which respectively the incident and the refracted rays make with this resultant or normal n. ρl, $\rho' l$, nl are the angles which three lines ρ, ρ', n make respectively with any assumed line l. As well as, if ρx, ρy, ρz; $\rho' x$, $\rho' y$, $\rho' z$; nx, ny, nz denote the angles which the two rays and the normal make respectively with three rectangular axes, x, y, z, we obtain [f]

$$\begin{cases} \cos\rho x + m\cos\rho' x = (\cos\rho n + m\cos\rho' n)\cos nx \\ \cos\rho y + m\cos\rho' y = (\cos\rho n + m\cos\rho' n)\cos ny \\ \cos\rho z + m\cos\rho' z = (\cos\rho n + m\cos\rho' n)\cos nz \end{cases} \tag{4}$$

We remark the direction of the incident ray is reverse in comparison with that one of refracted ray. Hence the (2) and (4) characterize the *algebraic aspects* of the Hamiltonian Optics.

1.2. *Analytic examen of the reflection and of the refraction*

At first we examine the reflection. Hamilton utilizes the symbol δx [instead of dx] in order to denote a point very near x. In the classical approach to the calculus of variations (see i.e.[8]), if for instance $f(x)$ is a function, that is a curve, $\delta f(x)$ represents a curve very close to $f(x)$. Therefore δx represents a straight line which passes by the point $P \equiv (x, y, z)$ of incidence, very close to a straight line by P , parallel to the axis x. A point P' infinitely near P has the following coordinates: $P' \equiv (x + \delta x, y + \delta y, z + \delta z)$ and because $\measuredangle nx = \measuredangle ny = \frac{\pi}{2}$, $z//n$, if P' is upon the mirror we have the following identity

$$\cos nx\delta x + \cos ny\delta y + \cos nz\delta z = 0 \tag{5}$$

[d]Ibid Hamilton says: "(2) is the analytic representation of the known law of reflection, and includes the whole theory of Catoptrics".

[e]See W.R.Hamilton, "Theory of systems of rays" (1828). Part Second *On ordinary systems of refracted rays,* Section XIV. *Analyrtic expression of the law of ordinary refraction.*

[f]Ibid Hamilton says: "(4) is the analytic expression of the known law of ordinary refraction, and includes the whole Theory of Dioptrics".

being $\cos nx = \cos ny = 0$, $\cos nz = 1$, and $\delta z \longrightarrow 0$. Of course, even if the operator δx is conceptually different than dx, according to the Lagrange $\delta-$calculus, they have interesting relations between them[g]. Moreover we write $\cos(\rho, x + \delta x) = \cos \rho x \delta x$ and likewise.

If one replaces (5) in (2) one obtains

$$\begin{aligned} &\cos \rho x \delta x + \cos \rho y \delta y + \cos \rho z \delta z + \\ &\cos \rho' x \delta x + \cos \rho' y \delta y + \cos \rho' z \delta z = 0 \end{aligned} \tag{6}$$

Now we consider a point $C \equiv (X, Y, Z)$ on ρ and a point $C' \equiv (X', Y', Z')$ on ρ', where $PC = |\rho|$, $PC' = |\rho'|$ and $|\rho| \neq |\rho'|$. Then if we take in account the Euler-Lagrange symbolism for the calculus of variations, we have

$$\delta \rho = \frac{\partial \rho}{\partial x} \delta x + \frac{\partial \rho}{\partial y} \delta y + \frac{\partial \rho}{\partial z} \delta z \tag{7}$$

Likewise

$$\delta \rho' = \left(\frac{\partial \rho'}{\partial x} \delta x + \frac{\partial \rho'}{\partial y} \delta y + \frac{\partial \rho'}{\partial z} \delta z \right) \tag{8}$$

Besides, if we put

$$\rho = \sqrt[2]{(X - x)^2 + (Y - y)^2 + (Z - z)^2} \tag{9}$$

and

$$\rho' = \sqrt[2]{(X' - x)^2 + (Y' - y)^2 + (Z' - z)^2} \tag{10}$$

from which

$$\begin{aligned} \frac{\partial \rho}{\partial x} &= \frac{1 \cdot 2(X - x)(-1)}{\sqrt[2]{(X - x)^2 + (Y - y)^2 + (Z - z)^2}} = \\ -\frac{(X - x)}{\rho} &= -\frac{\cos \rho x}{\rho} = -\cos \rho x \end{aligned} \tag{11}$$

Analogously for y, z and ρ'. From (611), we obtain

$$\delta \rho + \delta \rho' = 0 \tag{12}$$

The equation (12) represents the *Principle of least Action.* Hamilton says:

---

[g]Lagrange's δ-calculus was studied also by Euler (see in particular[8] (1766)). The relations between δ and d are the following (see also[3] pp. 237- 239):
1. The operators δ and d commute, that is $\delta d = d\delta$
2. The operator δ operates with the same rules as d
3. The operator δ and the integration operator commute, that is $\delta \int = \int \delta$
In[9] Euler defines δ so

$$\delta f(x, t) =_{def} dt \frac{\partial f}{\partial t_{|t=0}}$$

For instance $f(x, t) = f(x, 0) + tV(x)$ that is Euler embeds a given function $f(x)$ in a family $f(x, t)$

It [Principle] expresses that if the coordinates of the point of incidence were to receive any infinitely small variations consistent with the nature of the mirror, the bent path $\rho + \rho'$ would have its variation nothing; and if light be a material substance, moving with a velocity unaltered by reflection, this bent path $\rho + \rho'$ measures what in mechanics is called the Action, from the one assumed point to the other. [...]

[...] The formula (12) expresses that if we assume any two points, one on each ray, the sum of the distances of these two assumed points from the point of incidence, is equal to the sum of their distances from any infinitely near point upon the mirror.[...]

As Hamilton says, also Laplace obtained the equation (12).

Now we present the refraction case. If one considers three points respectively on the directions ρ, ρ' and n (which pass by the incidence point $P \equiv (x, y, z)$) and these three points are infinitely near P, the variations $\delta\rho$, $\delta\rho'$ and δn of the distances between P and these three points are proportional to the direction cosines of the lines ρ, ρ' and n. Hence the (3) becomes

$$\delta\rho + m\delta\rho' = (\cos\rho n + m\cos\rho' n)\delta n \tag{13}$$

When one takes P infinitely near the refracting surface one has $\delta n \to 0$, hence the (13) reduces itself to the *Principle of Least Action*, that is

$$\delta\rho + m\delta\rho' = 0 \tag{14}$$

where - as Hamilton says - "the distances on ρ and ρ' are positive if they are measured on the rays themselves, negative when on the rays produced".

From (14) we have

$$\rho + m\rho' = \text{ const.} \tag{15}$$

The class of surfaces which verify the (15) "was first discovered by Descartes [h] , on which account we shall call the *Cartesian Surfaces*. In the AppendixA we report the details of the Hamilton approach to define focal mirrors and focal refractors.

1.3. *On the Characteristic Functions*

The *Characteristic Function* depends on the particular combination of optical devices or instruments. It expresses a law of dependence of the final and initial directions of a linear path of light on the final and initial positions. Hamilton proposes two kinds of this function. For the case of reflection we consider the mirror as the plane x, y and the point $B \equiv (x_0, y_0, 0)$ as incident point. The path of light ρ' goes from an object $A \equiv (x', y', z')$ (source of light) to B , where the ray is reflected, and from B to $C \equiv (x, y, z)$ (i.e. an eye), so we have the reflected ρ. The initial ray ρ'

[h]See *Oeuvres*, VI, Paris 1902, pp.424-431

has the direction cosines α', β', γ' and the reflected ray ρ the direction cosines α, β, γ. In this case the characteristic function will can be

$$\begin{aligned} &\mathcal{V}(x, y, z; x', y', z') \\ &= \sqrt[2]{(x-x')^2 + (y-y')^2 + (z-z')^2} \end{aligned} \tag{16}$$

One can easily show that

$$\begin{aligned} \alpha = \frac{\partial \mathcal{V}}{\partial x} \; ; \; \beta = \frac{\partial \mathcal{V}}{\partial y} \; ; \; \gamma = \frac{\partial \mathcal{V}}{\partial z} \\ \alpha' = \frac{\partial \mathcal{V}}{\partial x'} \; ; \; \beta' = \frac{\partial \mathcal{V}}{\partial y'} \; ; \; \gamma' = \frac{\partial \mathcal{V}}{\partial z'} \end{aligned} \tag{17}$$

Hamilton establishes the variation of $\mathcal{V}$ by the following expression

$$\delta \mathcal{V} = \delta \int v ds \tag{18}$$

where v , which is a function of α, β, γ, is the corpuscolar velocity along the ray and s is the lenght of the optical path.

But it is possible to have, both for the reflection and for refraction together, an expression which individualizes the behaviour reflection-refraction of a optical path. So Hamilton asserts that when a sequence of rays, which starts from a source of light, are reflected and refracted any number of times as far as a final medium, we have a generalization of the (A.21), that is

$$\sum_{i=1}^{n} m_i \rho_i = \text{const.} \tag{19}$$

where $m_i = 1$ in the reflection case. Concerning this Hamilton holds the following proposition as an important Theorem of Optics:

When any system of homogeneous rays, issuing from a luminous point or from a perpendicular surface, has been any number of times modified by any combination of ordinarily reflecting and refracting surfaces, the final rays are cut perpendicularly by a series of surfaces, namely by the Surfaces of Constant Action

In this way the (19) can be considered a characteristic function.

Finally, in this context, the variational form of Fermat's principle is given by the following expression (see[10])

$$\delta \int_a^b n(x) ds = 0 \tag{20}$$

where $n(x)$ is the refraction index, s is the length of the optical path and a, b two fixed points in the space.

2. Hamilton's equations of a beam

Before considering an optical model for the betatronic dynamics, we shortly introduce the basic concept of the Hamiltonian dynamics of charge particles in circular accelerators. The Hamiltonian for the motion of a charged particle in a circular ring has the following expression in the paraxial approximation

$$H = \frac{p_x^2}{2} + \frac{p_y^2}{2} + V(x, y, s) \tag{21}$$

where $p_x = dx/ds$, $p_y = dy/ds$ and $s = v_0\, t$ denoting with v_0 the particle velocity. The potential is given by

$$V = \frac{1}{2}\frac{x^2}{R^2} + \frac{1}{2}\, K_1(s)(x^2 - y^2) - \frac{1}{6} K_2(s)(x^3 - 3xy^2) + \dots \tag{22}$$

The first contribution is due to the dipolar field and $R = mc\, v_0\gamma/eB_0$ is the radius of the circular orbit, the second term is the potential of the quadrupoles whose strength is piecewise contant with alternating signs, the third one is the contribution of the sextupoles and so on. The constant focusing approximation is obtained by replacing the piecewise constant quadrupolar strength with a constant one such that the focusing is uniform on the x and y directions in the transverse plane. This type of focusing is provided by solenoids. However a constant focusing model provides exactly the same Poincaré map if the ring is a sequence of m identical arcs having the same focusing and defocusing quadrupoles with a thin sextupole at the the beginning. One of these arcs, known as FODO cells, is schematically represented in figure 1 left. The stregth of the first sextupole of length ϵ can be written as $K_2(s) = k_2\delta_\epsilon(s)$ where $k_2 = \epsilon\, K_2$ is the integrated sextupolar gradient and $\delta_\epsilon(s) = 1/\epsilon$ if $0 < s < \epsilon$ and $\delta_\epsilon(s) = 0$ if $\epsilon < s < \ell$. On the lattice $\delta_\epsilon(s)$ is periodic with period ℓ and its $\epsilon \to 0$ limit is the periodic Dirac function with perod ℓ. This limit is taken keeping k_2 constant. The Poincaré map at $s = 0 \bmod \ell$ can be explicitly written and is given by

$$\begin{pmatrix} x_{n+1} \\ p_{x\,n+1} \end{pmatrix} = \mathsf{L}_x \begin{pmatrix} x_n \\ p_{x\,n} + \frac{1}{2}k_2\,(x_n^2 - y_n^2) \end{pmatrix} \qquad \begin{pmatrix} y_{n+1} \\ p_{y\,n+1} \end{pmatrix} = \mathsf{L}_y \begin{pmatrix} y_n \\ p_{x\,n} - k_2\, x_n y_n \end{pmatrix} \tag{23}$$

where the linear map L_x statisfies the constraint $|\,\mathrm{Tr}\,(\mathsf{L}_x)| < 2$ and so that it is conjugated to a rotation

$$\mathsf{L}_x = U_x \mathsf{R}(\omega_x)\mathsf{U}_x^{-1} \qquad \mathsf{U}_x^{-1} = \begin{pmatrix} \beta_x^{-1/2} & 0 \\ 0 & \beta_x^{1/2} \end{pmatrix} \begin{pmatrix} 1 & 0 \\ \alpha_x/\beta_x & 1 \end{pmatrix} \tag{24}$$

and the same expression holds for L_y. We perform the canonical change of coordinates $x' = x$, $p'_x = p_x + x\,\alpha_x/\beta_x$ and the same for y, p_y assuming that $\omega_x\beta_x = \omega_y\beta_y = \lambda$ where λ is comparable with ℓ though not equal to ℓ. The

map (3) written in the new momenta p'_x, p'_y, we still denote p_x, p_y, is the same as the Poincaré map at $s = 0 \bmod \lambda$ of the following Hamiltonian

$$H = \frac{p_x^2}{2} + \frac{p_y^2}{2} + \frac{x^2}{2\beta_x^2} + \frac{y^2}{2\beta_y^2} - \frac{k_2}{6}(x^3 - 3xy^2)\,\delta(s) \tag{25}$$

where $\delta(s)$ is the periodic δ function of period λ. We assume from now on that $\beta_x = \beta_y = \beta$ so that the quadratic Hamiltonian rotationally invariant. We perform the canonical transformation $x' = x\beta^{-1/2}$, $p'_x = \beta^{1/2}\,p_y$ and the same for y, p_y followed by the scaling with $\beta^{3/2}k_2/2$ for all the coordinates, we scale s with λ and scale the Hamiltonian according to

$$X = \frac{k_2}{2}\,\beta x \qquad P_x = \frac{k_2}{2}\,\beta^2\,p_x \qquad\qquad Y = \frac{k_2}{2}\,\beta y \qquad P_y = \frac{k_2}{2}\,\beta^2\,p_y$$

$$\sigma = \frac{s}{\lambda} \qquad\qquad \mathcal{H} = \ell\left(\frac{k_2}{2}\right)^2 \beta^3\,H \tag{26}$$

Such a transformation leaves the equations of motion invariant. In the new coordinates the scaled Hamiltonian reads

$$\mathcal{H} = \frac{\omega}{2}(P_x^2 + P_y^2 + X^2 + Y^2) - \frac{1}{3}\left(X^2 - 3\,XY^2\right)\delta(\sigma) \qquad \omega = \frac{\lambda}{\beta} \tag{27}$$

where $\delta(\sigma)$ is periodic of period 1. If $\omega \ll 1$ then the orbit of the Poincaré map at $\sigma = 0 \bmod 1$ is accurately interpolated by the orbit of the Hénon-Heiles Hamiltonian given by (27), where the δ function is replaced by 1. After further scaling $X = \omega X', P_x = \omega P'_x$ and $\mathcal{H} = \omega^3\mathcal{H}'$ the interpolating Hamiltonian

$$\mathcal{H}' = \frac{1}{2}\left({P'_x}^2 + {P'_y}^2 + {X'}^2 + {Y'}^2\right) - \frac{1}{3}({X'}^3 - 3X'{Y'}^2) \tag{28}$$

wallows to determine the stability boundary. Indeed this Hamiltonian has three saddle points $P'_x = P'_y = 0$ and $X' = -1/2, Y' = \pm\sqrt{3}/2$ and $X' = 1, Y' = 0$ where $\mathcal{H}' = 1/6$. The stability region is $\mathcal{H}' \le 1/6$. In the X', Y' plane the stability boundary is an equilateral triangle and the the circle ${X'}^2 + {Y'}^2 = 1/4$ is within it. The sphere of radius 1/2 given by ${P'_x}^2 + {P'_y}^2 + {X'}^2 + {Y'}^2 \le 1/4$ is within the stability region $\mathcal{H}' \le 1/6$. In the orginal coordinates the condition reads

$$x^2 + y^2 + \beta^2(p_x^2 + p_y^2) \le r_A^2 \qquad\qquad r_A = \frac{\omega}{k_2\beta} \tag{29}$$

We call r_A the dynamic aperture radius. The ellipsoid defined by (29) is within the stability region. The section with the (x, y) plane is a disc of radius r_A, with the p_x, p_y plane a disc of radius r_A/β and the section with the x, p_x or x, p_y planes an ellipse os semiaxis r_A and r_A/β, see AppendixB.

3. Hamilton's equations of rays

In geometrical optics the rays trajectories are the stationary solutions of the Fermat's functional

$$\mathcal{F} = \int_A^B n_{\text{ref}}(x, y, z)\, ds \tag{30}$$

where the endpoints are fixed, n_{ref} denotes the refraction index $n = c/v \geq 1$ with v is the light velocity in the medium. If the rays propagation is quasi rectilinear, introducing Cartesian coordinates with the z axis along the propagation direction, we parametrize the trajectory according to $x = x(z)$, $y = y(z)$ so that $ds = \sqrt{1 + x'^2 + y'^2}\, dz$ where $x' = dx/dz$, $y' = dy/dz$. The stationary solution satisfies the Euler-Lagrange equations with Lagrangian $L = n_{\text{ref}} \sqrt{1 + x'^2 + y'^2}$. The conjugate momenta are

$$p_x = n_{\text{ref}} \frac{x'}{\sqrt{1 + x'^2 + y'^2}} = n_{\text{ref}} \frac{dx}{ds} \qquad p_y = n_{\text{ref}} \frac{y'}{\sqrt{1 + x'^2 + y'^2}} = n_{\text{ref}} \frac{dy}{ds} \tag{31}$$

The Hamiltonian is

$$H_{\text{ray}} = x' p_x + y' p_y - L = -\frac{n_{\text{ref}}}{\sqrt{1 + x'^2 + y'^2}} = -\sqrt{n^2_{\text{ref}} - p_x^2 - p_y^2} \tag{32}$$

If n depends only on z then the momenta are invariant and this corresponds to the Snell law of refraction. Indeed consider a ray propagating on the x, z plane and let θ be the the angle the tangent to ray forms with the z axis then $p_x = n_{\text{ref}}\, dx/ds = n_{\text{ref}} \sin\theta$ is constant along the ray trajectory. It is convenient to set

$$n^2_{\text{ref}} = n_0^2 (1 - 2V) \tag{33}$$

and to perform the scaling $H/n_0 \to H$, $p_x/n_0 \to p_x$, $p_y/n_0 \to p_x$ so that the Hamiltonian becomes

$$H = -\sqrt{1 - 2\left(\frac{p_x^2 + p_y^2}{2} + V(x, y, z)\right)} \tag{34}$$

We consider the case of rays propagating in a cylindrical wave guide of radius r_w, If the rays propagate very close to wave guide axis z we can use the paraxial approximation. If $|p_x| \ll 1$, $|p_y| \ll$ and $|V| \ll 1$ the Hamiltonian is approximated by

$$H = -1 + \frac{1}{2}(p_x^2 + p_y^2) + V(x, y, s) \tag{35}$$

The variation of the refraction must be small to allow a paraxial ray propagation. In general given a potential V we may find a medium with refractive index n according to (33), provided that $V < 1/2$ in the region of interest. This condition allows to find a n_0 such that $n \geq 1$.

Rather than the propagation of a single ray is convenient to consider also the propagation of a ray bundle. Letting $\rho_0(x, p_x, y, p_y)$ be the initial distribtion at $s = 0$ of

the rays budle the distribution $\rho(x, p_x, y, p_y, s)$ at any further section s of the wave guide satisfies the Liouville equation

$$\frac{\partial \rho}{\partial s} + [\rho, H] = 0 \tag{36}$$

where $[\,.\,,\,.\,]$ denotes the Poisson Bracket.

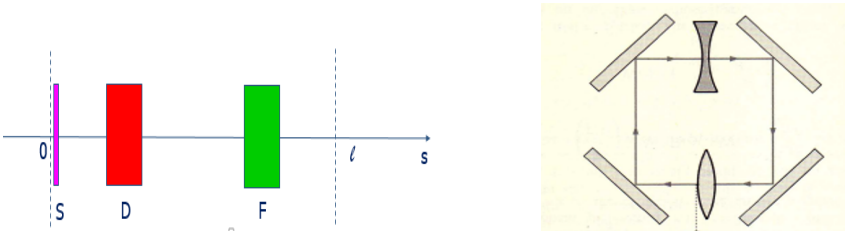

Fig. 1. Left frame: FODO cell with thin sextupole. Right frame: optical system with four mirrors and two lenses simulating a FODO cell

3.1. *Mirror and lenses*

An optical analogue of the accelerating ring with identical FODO cells can be achived with mirrors and lenses. In the case of a single cell $m = 1$ a possible arrangement is shown in figure 1 right. A full correspondence is achieved in the x, p_x phase plane if the beam is flat, the reference orbit is a square obtained with four thin dipoles, the quadrupoles are thin and the rays propagate in a plane orthogonal to the mirrors and to the the thin focusing and defocusing lenses. The inclusion of a thin sextupole and an equivalent lens allows a perfect correspondence to hold also in the nonlinear case. An experiment was performed[6,7] and a good agreement with the basic theory was found. In order to have a correspondence in the 4D phase space x, p_x, y, p_y we need lenses which are convergent in one plane and divergent on the other and non nonlinear lenses reproducing a sextupolar kick. A serious problem with this setup is the intensity loss due to the propagation in the air, to reflections and to the crossing of the lenses. A vacuum chamber would help to reduce the losses, but the complexity and cost of the system would increase considerably

3.2. *The waveguide analogue*

An alternative optical model, whose rays are just the trajectories of a particle with Hamiltonian given by equation (25), is provided by a straight cilindrical waveguide with axis along z and of radius r_w, whose refraction index n is given by equation (33). Letting $V_{\max} = \max V(x, y, z)$ for $r < r_w$ and any z, the condition $n_0^2 >$

$(1-2V_{\max})^{-1}$ must be satisfied, which implies $V_{\max} < 1/2$. We consider an axially symmetric model in which $\beta_x = \beta_y$ so that refraction index depends only on the radial coordinates, except for short sections corresponding to the sextupoles. Using polar coordinates the rays the Hamiltonian (32) reads

$$H = \sqrt{1 - p_r^2 - p_\phi^2/r^2 - r^2/\beta^2} \tag{37}$$

if the sextupoles are absent. In this case p_ϕ is a first integral of motion. The symmetric waveguide where $n = n(r)$ is the simplest to implement. The presence of sextupolar insertions renders the use of Cartesian coordinates more convenient. Cylindrical coordinates were used for a model where n^2 is quadratic in r^2 rather than r so that H has an elliptic and an hyperbolic critical point in the r, p_r phase plane[11]. The sextupolar insertion modeled as kick in (25) has to be replaced with a section of finite lengh ϵ so that the condition $2V_{\max} < 1$ can be satisfied. For the paraxial approximation to hold we require that $p_x^2 + p_y^2 \ll 1$ and $|V| \ll 1$ for $r \le r_w$. Recalling that the potential $V(x, y, s)$ is a periodic function of period λ, the first focusing section $\epsilon < s < \lambda$ we have $2V = r^2/\beta^2$ and the paraxial approximation holds if $r_w \ll \beta$. In the first sextupolar intertion insertion $0 < s < \epsilon$ we have

$$2V = -\frac{K_2}{3}(x^3 - 3xy^2) = \frac{k_2}{3\epsilon}\, r^3(3\cos\theta - 4\cos^3\theta) \tag{38}$$

We use of polar coordinates to show that $3\cos\theta - 4\cos^2\theta$ varies between -1 and 1 reached for $\cos\theta = -1/2$ and $\cos\theta = 1/2$ respectively. As a consequence the paraxial approximation holds provided that $k_2 r_w^3/(3\epsilon) \ll 1$.

We should not forget that some ray tajectories could reach the waveguide boundary $r = r_w$ and reflect on it. When this occurs we have the dynamics of a billiard and it is no longer described by (34) or (35). In this case the correspondence between the rays in the waveguide and the particles in the ring is lost.

Except for the short nonlinear insertions which change the rays directions p_x, p_y, the trajectories in the (x, p_x) and (y, p_y) phase planes and in the (x, y) plane are arcs of ellipses. After the canonical change of coordinates $x' = \beta^{-1/2}\, x,\ p'_x = \beta^{1/2}\, p_x$, $y' = \beta^{-1/2}\, y,\ p'_y = \beta^{1/2}\, p_y$ the trajectories are arcs of circles in the phase planes but in the x', y' plane the orbits are still arcs of ellipses. Letting $x_n, p_{x\,n}, y_n, p_{y\,n}$ the phase space coordinates after the n-th sextupolar insertion $(n-1)\lambda < s < (n-1)\lambda + \epsilon$ the x, y coordinates in the interval $(n-1)\lambda + \epsilon < s < n\lambda$ are given by

$$x(s) = x_n\, \cos\phi + \beta p_{x\,n}\, \sin\phi \qquad y(s) = y_n\, \cos\phi + \beta p_{y\,n}\, \sin\phi \tag{39}$$

where $\phi = \big(s - (n-1)\lambda - \epsilon\big)/\beta$. No reflections occur as long as

$$x^2(s) + y^2(s) \le x_n^2 + y_n^2 + \beta^2(p_{x\,n}^2 + p_{y\,n}^2) + 2\beta(|x_n|\,|p_{x\,n}| + |y_n|\,|p_{y\,n}|) \le$$

$$\le 2\left(x_n^2 + y_n^2 + \beta^2(p_{x\,n}^2 + p_{y\,n}^2)\right) \le r_w^2 \tag{40}$$

where we used the inequality $2|a|\,|b| \le a^2 + b^2$.

We resume the conditions for an optical experiment on a waveguide of radius r_w which simulates the motion of particle in a ring with identical FODO cells with a sextupole, figure 1 left. The linear part of the FODO cell gives a phase advance ω and the beta function β at the endpoints of the cell. The nonlinear part is a thin sextupole at the beginning of the cell with integrated gradient $k_2 = \ell_{\text{sex}}\ K_2$. In the waveguide it is replaced by a section of length ϵ with the same integrated gradient K_2 and gradient k_2/ϵ

$$n^2_{\text{ref}} = n_0^2 \times \begin{cases} 1 + \dfrac{k_2}{3\epsilon}(x^3 - 3xy^2) & 0 < s < \epsilon \\ \\ 1 - \dfrac{x^2+y^2}{\beta^2} & \epsilon < s < \ell \end{cases} \tag{41}$$

where $(\ell - \epsilon) = \beta\,\omega$. We choose $\epsilon \ll \ell$ so that the non linear contribution is very close to a kick and $\ell \simeq \omega\beta$. The first condition we impose is $|V| \ll 1$ for the paraxial approximation to hold, and therefore we may choose n_0 rather close to 1, fors instance $n_0 = 1.2$. The second condition to impose is on the dynamic aperture. We rquire that $r_w < r_A$ where the dynamic aperture radius is given by (29) in the approximation $\omega \ll 1$. The estimate (29) is still reliable up to $\omega \simeq 1$. The Hamiltonian describing the rays trajectories in a waveguide with refraction index diven by (41) in the paraxial approximation is given by

$$H = \frac{p_x^2}{2} + \frac{p_y^2}{2} + \frac{x^2+y^2}{2\beta^2}(1 - \Theta_\epsilon(s)) - \frac{k_2}{6\epsilon}(x^3 - 3xy^2)\,\Theta_\epsilon(s) \tag{42}$$

where $\Theta_\epsilon(s)$ is a periodic step function of period λ such that $\Theta_\epsilon(s) = 1$ for $0 < s < \epsilon$ and $\Theta_\epsilon(s) = 0$ for $\epsilon < s < \lambda$. This Hamiltonian describes the rays trajectories but since $\epsilon/\lambda \ll 1$ the orbits of its Poincaré map at $s = 0 \bmod \lambda$ are well approximated by the orbits of the Poincaré map of Hamiltonian ((25) which after the scaling (26) leading to the Hamiltonian (27) are precisely the orbits of 4D Hénon map given by

$$\begin{pmatrix} X_{n+1} \\ P_{x\,n+1} \end{pmatrix} = \mathsf{R}(\omega) = \begin{pmatrix} X \\ P_{x\,n+1} + X_n^2 - Y_n^2 \end{pmatrix} \quad \begin{pmatrix} Y_{n+1} \\ P_{y\,n+1} \end{pmatrix} = \mathsf{R}(\omega) = \begin{pmatrix} X \\ P_{x\,n+1} - 2X_n\,Y_n \end{pmatrix} \tag{43}$$

The choice we make to insure that we are within the stability region is

- $$r_w < r_A = \frac{\lambda}{2k_2\beta^2}$$

The paraxial appromation requires that

- $$\frac{r_w}{\beta} \ll 1 \qquad \frac{k_2}{3}\,\frac{r_w^3}{\epsilon} < \frac{1}{3}\,\frac{\lambda}{\epsilon}\,\left(\frac{r_w}{\beta}\right)^2 \ll 1$$

and the reflections are avoided provided that

$$\bullet\bullet\bullet \qquad x_n^2 + y_n^2 + \beta^2(p_{x\,n}^2 + p_{y\,n}^2) \leq \frac{r_w^2}{2}$$

We have taken into account (29) with $\omega = (\lambda - \epsilon)/\beta \simeq \lambda/\beta$, The second condition in $\bullet\bullet$ puts a lower bound, easy to satisfy, on the thickness of the waveguide section corresponding to the sextupole nonlinearity $\epsilon/\ell \geq r_w/(6\beta)$. Choosing initial condtions according to $\bullet\bullet\bullet$ for $n = 0$ we are surely within the stability boundary since $r_w < r_A$ and if the condition is fulfilled for any n we are sure that reflections do not occur. In the scaled coordinates X, P_x, Y, P_y where the orbit is determined by the Hénon map, the dynamic aperture radius r_A becomes $R_A = \omega/2$ and r_w becomes $R_w = (r_w/r_A)\omega/2$. For simplicity we consider the orbits in the X, P_x obtained by choosing $Y_0 = P_{y\,0} = 0$. In this case if $X_n^2 + P_{x\,n}^2 < R_w^2$ the absence of reflections is insured, since the orbits between two kicks are arcs of circle. We chose the initial conditions in a disc $X_0^2 + P_{x\,0}^2 < R_0^2$ where R_0 is chosen in such a way that reflections are avoided at any further iteration n. An example for $\omega = 1.288$ with $R_w = 0.9R_A$ and $R_0 = 0.55R_A$ is shown in figure 2 left.

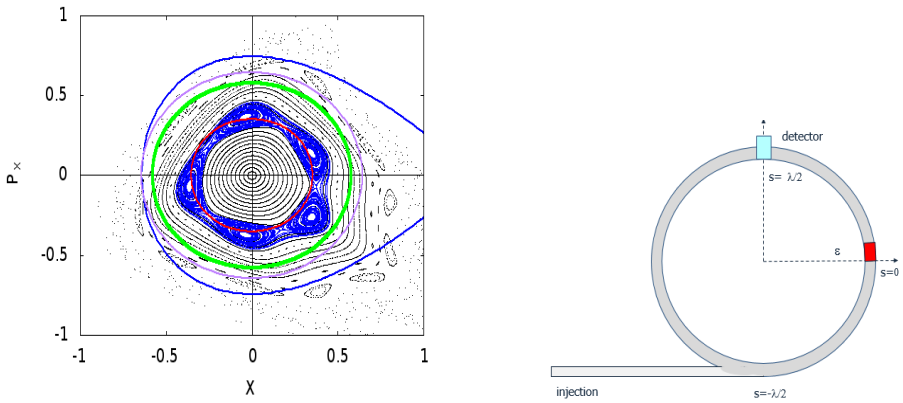

Fig. 2. Left panel: orbit of the Hénon map in the X, P_x phase plane for $Y = P_y = 0$ with $\omega = 1.288$ and $\nu = \omega/2\pi = 0.205$. The dynamic aperture approximation obtained from the Hamiltonian (28) $P_x = \pm(1-X)\sqrt{(1+2X)/3}*$ is the Blue curve, the disc with dynamic aperture radius $R_A = \omega/2$ is purple, the disc of radius $R_w = 0.9R_A$ is green and the disc of initial conditions $R_0 = 0.55R_A$ is read. The orbits with the initial conditions on the circle of radius R_0 are blue.

As a specific example we choose a lattice of the SESAME ring see `http://www.sesame.org.jo/sesame/images/sesame-publications/Magnets.pdf`.
The quadrupoles have $K_1 = 3$ m^{-2} and lenght $\ell_Q = 0.2$ m, the tolal lenght of the cell is $L = 4$m. This gives $\omega = 1.306$, $\nu = 0.208$ and $\beta = 3.4$ m so that $\lambda = \omega\beta = 4.4$ m. The sextupoles have a gradient $K_2 = 50$ m^{-3} and length 0.15 m so that the

integrated gradient is $k_2 = 7.5$ m^{-2}. We choose a unique stronger setupole of integrated gradient $k_2 = 20$ m^{-2} to have a dynamic aperture radius $r_A \simeq 2$ cm and we choose accordingly $r_w = 1$ cm. Another test case is with shorter quadrupoles $\ell_Q = 1$ cm and we get $\omega = 0.6$, $\nu = 0.095$ $\beta = 6.8$ so that $\lambda = \omega\beta = 4$ m. . In this case we choose $k_2 = 4.5$ m^{-2} to have about the same aperture $r_A \sim 2$ cm. The lower value of ω renders the estimates of the dynamic aperture are more accurate.

One may consider two different arrangemets: a long straight waveguide made up of N identical sections of lenth ℓ. In this case the injection is simple as well as the final recording but one can only obtain the map from the inital to the final condition including the rays budles rather than single rays. More interesting is the arrangement of the waveguide of lengh ℓ as closed circular loop. The injection can be made with gluing the circular waveguide with another waveguide tanget to it right at $s = -\lambda/2$ for instance, inserting a detecting system at $s = \lambda/2$ driven by two plates capable of recording the rays transverse coordinates x, y from which the ray direction given by p_x, p_y can be obtained, see figure 2. Since for a a tipical length $\lambda = 3$ m the time delay between two passes is 10 ns, the pass by pass detection might be challenging. The feasibility and cost of such an experiment require further investigation.

3.3. *Wave guides and cavities with reflections*

Another interesting dynamical model is offered by the waveguides in which the light reflects at small angles and can propagate over long distances. Wave cavities have also beam considered in which the light propagates in the interior of a closed reflecting domain and can escape when the incidence angle is below a critical value. We distinguish between plane waveguides and plane resonant cavities. The simplest integrable example of wave guide is given by two parallel lines at distance ℓ, the lowest of which we assume to be the x axis. The simplest example of cavity is a circle of radius R. In the former case letting θ be the angle the ray forms with the x axis and denoting with (x_n, θ_n) the of the coordinates after n reflections starting with x_0, θ_0 the map is simply

$$\theta_{n+1} = \theta_n \qquad x_{n+1} = x_n + 2\ell \cot\theta_n \tag{44}$$

whereas in the case of the circle denoting with s_n the arc between two susequent reflections and θ the angle the ray forms with the tangent at the reflection point, the map for (θ_n, s_n) is

$$\theta_{n+1} = \theta_n \qquad s_{n+1} = s_n + 2R\,\theta_n \tag{45}$$

For simplicity we assume $\ell = R = 1$ from now on. One or both the parallel planes of the rectangular waveguide can include corrugations of arbitrary depths [12]. In this case, the particle dynamics can deviate substantially from a ballistic motion and become diffusive with the increasing depth of corrugation [13]. The geometry of

the corrugated waveguide considered in this contribution is shown in Figure 3. The collision map of particles bouncing within a corrugated waveguide can be derived also in this case through simple geometrical considerations. The equation for the corrugated profile is

$$y = 1 + \epsilon f(x) \tag{46}$$

and the map of two subsequent reflections with the lower boundary $y = 0$ is still area preserving and can be determined as follows. Starting from $x = x_n$ with an

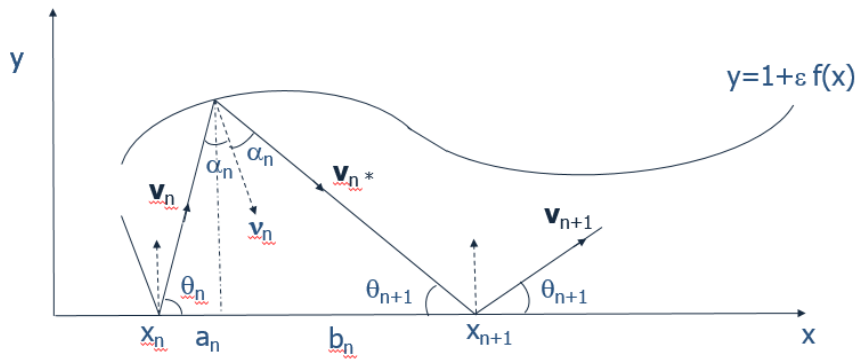

Fig. 3. Geometry of reflections in a plane waveguide

angle $\theta_n < \pi/2$ we hit the upper boundary at $x_* = x_n + a_n$, $y_* = 1 + \epsilon(x_n + a_n)$. To determine a_n we notice that the velocity of the ray is $\mathbf{v} = c(\cos\theta_n, \sin\theta_n)$. Choosing $c = 1$ time τ between the rections at $(x_n, 0)$ and x_*, y_* is such that

$$a_n = \tau\cos\theta_n \qquad\qquad 1 + \epsilon f(x_n + a_n) = \tau\sin\theta_n \tag{47}$$

After solving the second implicit equation to determine τ we obtain a_n. The next reflection with the $x = 0$ axis occurs at $x_{n+1} = x_n + a_n + b_n$. The triangle with vertices $(x_n, 0)$, (x_*, y_*), $(x_{n+1}, 0)$ has angles $\theta_n, 2\alpha_n, \theta_{n+1}$, see figure 2, where α_n is the angle between the normal $\boldsymbol{\nu}$ at the upper boundary at (x_*, y_*) and the reflected ray, which is the same as the incident angle. As a consequence we have

$$\theta_{n+1} = \pi - \theta_n - 2\alpha_n \tag{48}$$

The normal $\boldsymbol{\nu}_n$ to the corrugated surface, see figure 3, is given by

$$\boldsymbol{\nu}_n = \frac{(\epsilon f'(x),\ -1)}{\sqrt{1 + \epsilon^2 f'^2(x)}} \tag{49}$$

The incidence and reflection angle α_n, see figure 3, is given by

$$\cos(\alpha_n) = \boldsymbol{\nu} \cdot \mathbf{v}_{n\,*} = -\boldsymbol{\nu} \cdot \mathbf{v}_n = \frac{\sin\theta_n - \epsilon f'(x_n + \tau\cos\theta_n)\cos\theta_n}{\sqrt{1 + \epsilon^2\, f'^2(x_n + \tau\cos\theta_n)}} \tag{50}$$

The final expression for the map is obtained observing that $x_{n+1} = x_n + a_n + b_n$ where $b_n = y(x_n + a_n)\cot\theta_{n+1}$ and $y(x_n + a_n) = \tau\sin\theta_n$ from (47). Introducing the angle $\beta_n = \pi/2 - \alpha_n$ so that $\sin\beta_n = \cos\alpha_n$ given by (50) and taking equation (48) into account we have

$$\begin{cases} \theta_{n+1} = 2\beta_n - \theta_n \\ x_{n+1} = x_n + \tau\sin\theta_n\ (\cot\theta_n + \cot\theta_{n+1}) \end{cases} \tag{51}$$

where τ is the solution of the implicit equation (47). This is the map when the ray moves forward along the positive x axis as shown by figure (3). When the rays invert the motion under some conditions $\beta_n = \pi/2 + \alpha_n$ and to avoid a cumbersome discussion is is conveneint to consider that the velocity vector after the reflection on the corrugated boundary is $\mathbf{v}_{n\,*} = (\cos\theta_{n+1},\, -\sin\theta_{n+1})$ and after the subsequent reflection on the x axis it becomes $\mathbf{v}_{n+1} = (\cos\theta_{n+1},\, \sin\theta_{n+1})$. The law of reflection imposes

$$\mathbf{v}_{n\,*} = \mathbf{v}_n - 2\boldsymbol{\nu}_n\,(\boldsymbol{\nu}_n \cdot \mathbf{v}_n) = \mathbf{v}_n\ + 2\,\boldsymbol{\nu}_n\ \cos\alpha_n \tag{52}$$

and the map, valid in any possible condition reads

$$\begin{cases} \theta_{n+1} = \mathrm{acos}\left(\cos\theta_n + 2\ \dfrac{\epsilon f'(x_n + \tau\cos\theta_n)}{\sqrt{1 + \epsilon^2\, f'^2(x_n + \tau\cos\theta_n)}}\ \cos\alpha_n\right) \\ \\ x_{n+1} = x_n + \tau\sin\theta_n\ (\cot\theta_n + \cot\theta_{n+1}) \end{cases} \tag{53}$$

Remark that for $\epsilon = 0$ we have $\theta_{n+1} = \theta_n$ and from equation (47) it follows that $\tau\sin\theta_n = 1$ so that the integrable map (44) is recovered. For $\epsilon \ll 1$ a first order expansion can be written[14,15]. We notice that if $f(x) = -x^2/2$ for $-a < x < a$ with $a < 1$ then for initial condtions $|\pi/2 - \theta_0| \ll 1$ and $|x_0| \ll 1$ the map is quasi integrable and the orbits in the phase space x, θ are ellipses since the boundary is a concave mirror which has a focusing effect. If $f(x) = x^2/2$ the boundary is convex mirror which has a defocusing affect. In this case the orbits in phase space close to the fixed point $0, \pi/2$ belong to arcs of hyperbolae. For a periodic perturbation such as $f(x) = \cos(x)$ the point $(0, \pi/2)$ is an elliptic fixed point, wheres $(\pm\pi, \pi/2)$ is an hyperbolic fixed point. In Figure 4 we show the orbits of the map for $f(x) = \cos(x)$. In a cavity the rays reflect on the boundary and if the cavity is a stadium formed by two half circles and two parallel lines the trajectories are chaotic, as shown by the Poincaré map[16]. The waveguide and the cavity can be extended to the full 3D space where the boudaries are 2D surfaces. In this case the reflection map is a 4D symplectic map in the Lagrange coordinates (q_1, q_2) of the reflecting surface

and the angles (θ_1, θ_2) defining the ray direction at the reflection point. Starting from integral models such as two parallel planes or a sphere quasi integrable and non integrable models can be built by corrugating the surfaces. In the literature

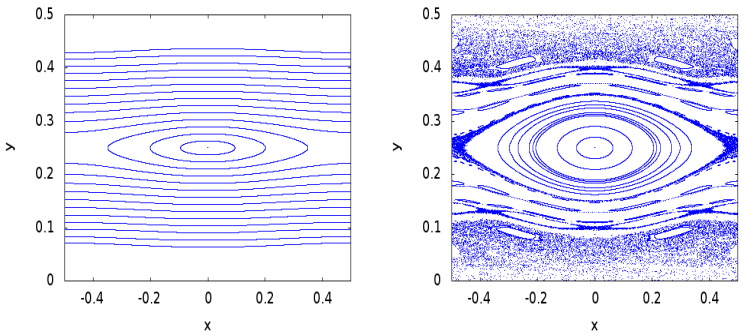

Fig. 4. Left side: orbits of the map (53) for $f(x) = \cos(x)$ and $\epsilon = 0.02$. The coordinates are $x' = x/(2\pi)\text{mod}1$ we still denote by x and $y = \theta/(2\pi)$. Right side: the same for $\epsilon = 0.1$

models of waveguides have been proposed [17] and experimentally the chaotic behavior of rays in cavities was used to extract intense beams when the incidence angle overcomes the critical value [18] also using semi-classical methods [19]. More generally, wave chaos based models of the propagation of acoustics wave have been derived to ray trace and advance densities of rays within billiards with arbitrary boundary geometry [20]. Furthermore, electromagnetic wave propagation within complex and multiply connected cavities have been described in terms of scattering matrix statistics, developed using random matrix theory (RMT) as well as semi-classical methods to describe cavity eigen-energy and eigen-function distributions respectively [21].

4. Conclusions

We hve examined the correspondence between the motion of a charged particle and the propagation of a ray in a medium with variable refraction index starting from the historical perspective. Rather than an optical arrangement based on mirrors and lenses as previously suggested and experimentally tested, we have examined a different setup based on an optical fiber with a radially increasing refraction index to simulate the linear betatronic motion and thin non linear insertions to simulate the nonlinear effect of a sextupole. We show that a fiber arranged as a circular ring could actually simulate the basic cell of a symmetric circular accelerator. If the difficulties concerning the injection and detection and be solved this sistem might provide and analogical simulation of the betatronic motion complementary to numerical simulations.

Appendix A. Focal mirrors and focal refractors

In order to find a mirror which reflects to a given focus the rays of a given source, we have to consider the following differential equation

$$(\alpha + \alpha')dx + (\beta + \beta')dy + (\gamma - \gamma')dz = 0 \tag{A.1}$$

where x, y, z are the coordinates of the mirror. It derives from (6) when one puts $\cos\rho x = \alpha$, $\cos\rho' x = \alpha'$, $\cos\rho y = \beta$, $\cos\rho' y = \beta'$, $\cos\rho z = \gamma$, $\cos\rho' z = \gamma'$ and dx instead of δx etc. Each α, β, γ, α', β', γ' is a function of x, y, z. α, β, γ depend on the nature of the source of light and α', β', γ' depend on the focus position. "The integral of (A.1) will represent an infinite number of different mirrors, each of which possess the property of reflecting to a given focus, the rays of the given system [source], and which for that reason I [Hamilton] shall call *focal mirrors*".

Now we want to know when the equation (A.1) is integrable. This equation, in the first member, is composed by two parts, so

$$\alpha' dx + \beta' dy + \gamma' dz \tag{A.2}$$

and

$$\alpha dx + \beta dy + \gamma dz$$

The part $\alpha' dx + \beta' dy + \gamma' dz$ is always an exact differential. In fact, if $F \equiv (X', Y', Z')$ is a assigned focus, by ρ' we denote the distance between the focus F and the incidence point $P \equiv (x, y, z)$. So we have

$$\begin{aligned} X' - x &= \alpha'\rho' \\ Y' - y &= \beta'\rho' \\ Z' - z &= \gamma'\rho' \end{aligned} \tag{A.3}$$

From (A.3) one derives $\rho' = \frac{X'-x}{\alpha'}$, etc., and from which

$$d_x\left(\frac{X'-x}{\alpha'}\right) = -\frac{1}{\alpha'}dx = d\rho'$$

etc.

and

$$dx = -\alpha' d\rho' \tag{A.4}$$

etc.

If we replace (A.4) in the first of (A.2) we obtain

$$\begin{aligned} &\alpha'(-\alpha')d\rho' + \beta'(-\beta')d\rho' + \gamma'(-\gamma')d\rho' \\ &= \alpha' dx + \beta' dy + \gamma' dz = -d\rho' \end{aligned} \tag{A.5}$$

because, by virtue of a property of direction cosines,

$$\alpha'^2 + \beta'^2 + \gamma'^2 = 1 \tag{A.6}$$

Hence the (A.5) establishes that $\alpha' dx + \beta' dy + \gamma' dz$ is an exact differential. If we take into account a well known theorem which characterizes (iff) the exact differentials, we can have the following equation

$$\alpha' \left(\frac{\partial \beta}{\partial x} - \frac{\partial \gamma}{\partial y} \right) + \beta' \left(\frac{\partial \gamma}{\partial x} - \frac{\partial \alpha}{\partial z} \right) + \gamma' \left(\frac{\partial \alpha}{\partial y} - \frac{\partial \beta}{\partial x} \right) = 0 \tag{A.7}$$

which is verified because, in virtue of recalled theorem, we have

$$\left(\frac{\partial \beta}{\partial z} - \frac{\partial \gamma}{\partial y} \right) = \left(\frac{\partial \gamma}{\partial x} - \frac{\partial \alpha}{\partial z} \right) = \left(\frac{\partial \alpha}{\partial y} - \frac{\partial \beta}{\partial x} \right) = 0 \tag{A.8}$$

But in order to find the integral of the (A.1) it is necessary establishes if we have also

$$\alpha \left(\frac{\partial \beta}{\partial z} - \frac{\partial \gamma}{\partial y} \right) + \beta \left(\frac{\partial \gamma}{\partial x} - \frac{\partial \alpha}{\partial z} \right) + \gamma \left(\frac{\partial \alpha}{\partial y} - \frac{\partial \beta}{\partial x} \right) = 0 \tag{A.9}$$

Hamilton expounds the following reasoning. He says the functions (with three independent variables x, y, z) α, β, γ "will not vary when the coordinates of the incidence point $P \equiv (x, y, z)$ receive any variations δx, δy, δz proportional to those cosines α, β, γ, because then the point $(x+\delta x, y+\delta y, z+\delta z)$ will belong to the same incident ray, as the point $P \equiv (x, y, z)$". That is we have the following equations

$$\begin{aligned} \delta\alpha &= \alpha \frac{\partial \alpha}{\partial x} + \beta \frac{\partial \alpha}{\partial y} + \gamma \frac{\partial \alpha}{\partial z} = 0 \\ \delta\beta &= \alpha \frac{\partial \beta}{\partial x} + \beta \frac{\partial \beta}{\partial y} + \gamma \frac{\partial \beta}{\partial z} = 0 \\ \delta\gamma &= \alpha \frac{\partial \gamma}{\partial x} + \beta \frac{\partial \gamma}{\partial y} + \gamma \frac{\partial \gamma}{\partial z} = 0 \end{aligned} \tag{A.10}$$

Moreover, if one differentiates $\alpha^2 + \beta^2 + \gamma^2 = 1$ one obtains

$$\alpha d\alpha + \beta d\beta + \gamma d\gamma = 0$$

and as well

$$\begin{aligned} \alpha \frac{\partial \alpha}{\partial x} + \beta \frac{\partial \beta}{\partial x} + \gamma \frac{\partial \gamma}{\partial x} &= 0 \\ \alpha \frac{\partial \alpha}{\partial y} + \beta \frac{\partial \beta}{\partial y} + \gamma \frac{\partial \gamma}{\partial y} &= 0 \\ \alpha \frac{\partial \alpha}{\partial z} + \beta \frac{\partial \beta}{\partial z} + \gamma \frac{\partial \gamma}{\partial z} &= 0 \end{aligned} \tag{A.11}$$

Now, comparing (A.10) with (A.11) it results

$$\alpha \frac{\partial \alpha}{\partial x} + \beta \frac{\partial \alpha}{\partial y} + \gamma \frac{\partial \alpha}{\partial z} = \alpha \frac{\partial \alpha}{\partial x} + \beta \frac{\partial \beta}{\partial x} + \gamma \frac{\partial \gamma}{\partial x} = 0$$

that is

$$\beta \left(\frac{\partial \alpha}{\partial y} - \frac{\partial \beta}{\partial x} \right) = \gamma \left(\frac{\partial \gamma}{\partial x} - \frac{\partial \alpha}{\partial z} \right) = 0 \tag{A.12}$$

Likewise from

$$\alpha\frac{\partial\gamma}{\partial x}+\beta\frac{\partial\gamma}{\partial y}+\gamma\frac{\partial\gamma}{\partial z}=\alpha\frac{\partial\alpha}{\partial z}+\beta\frac{\partial\beta}{\partial z}+\gamma\frac{\partial\gamma}{\partial z}=0$$

we have

$$\alpha\left(\frac{\partial\gamma}{\partial x}-\frac{\partial\alpha}{\partial z}\right)=\beta\left(\frac{\partial\beta}{\partial z}-\frac{\partial\gamma}{\partial y}\right)=0 \tag{A.13}$$

From (A.12) and (A.13) we have

$$\left(\frac{\partial\beta}{\partial z}-\frac{\partial\gamma}{\partial y}\right)=\left(\frac{\partial\gamma}{\partial x}-\frac{\partial\alpha}{\partial z}\right)=\left(\frac{\partial\alpha}{\partial y}-\frac{\partial\beta}{\partial x}\right)=0 \tag{A.14}$$

Therefore, in virtue by the previous recalled theorem also $\alpha dx+\beta dy+\gamma dz$ is an exact differential. Hence the equation (A.1) is integrable.

The conditions (A.14), according to another theorem which concerns the exact differentials, geometrically have the following meaning: "These conditions express - as Hamilton says - that the rays of the incident system [source] are cut perpendicularly by a series of surfaces, having for equation"

$$\int(\alpha dx+\beta dy+\gamma dz)=\text{const.} \tag{A.15}$$

Now we consider a point $Q\equiv(X,Y,Z)$ in which an incident ray cuts one of the surfaces (A.15), let $P\equiv(x,y,z)$ a point of incidence and ρ the dinstance between Q and P. Then we shall have

$$\begin{aligned} X-x&=\alpha\rho \\ Y-y&=\beta\rho \\ Z-z&=\gamma\rho \end{aligned} \tag{A.16}$$

By means of the same procedure for (A.5) we obtain

$$\alpha dx+\beta dy+\gamma dz=-d\rho \tag{A.17}$$

where in this case we have $\alpha dX+\beta dY+\gamma dZ=0$.

So the differential equation of the mirror (A.1), from (A.5) and (A.17) becames

$$d\rho+d\rho'=0 \tag{A.18}$$

which has as integral the equation

$$\rho+\rho'=\text{const.} \tag{A.19}$$

The (A.19) "expresses that the whole bent path traversed by the light in going from the perpendicular surface (A.15) to the mirror, and from the mirror to the focus, is of a constant length, the same for all the rays. In this interpretation - as Hamilton says - of the integral (A.19) we have supposed the distances, ρ and ρ' positive".

In the case of refraction (refractors, in particular lens) we have:

α, β, γ (functions of x, y, z) as direction cosines of the incident ray ρ, $P \equiv (x, y, z)$ as point of incidence of ρ; α', β', γ' (functions of x, y, z) as direction cosines of the refracted ray ρ'(which passes through the point $P \equiv (x, y, z)$, on the lens, and through the focus $F \equiv (X', Y', Z')$). Hamilton arrives to the following differential equation:

$$\begin{aligned} &\alpha\left(\frac{\partial\beta}{\partial z}-\frac{\partial\gamma}{\partial y}\right)+\beta\left(\frac{\partial\gamma}{\partial x}-\frac{\partial\alpha}{\partial z}\right)+\gamma\left(\frac{\partial\alpha}{\partial y}-\frac{\partial\beta}{\partial x}\right)+ \\ &+m\alpha'\left(\frac{\partial\beta}{\partial z}-\frac{\partial\gamma}{\partial y}\right)+m\beta'\left(\frac{\partial\gamma}{\partial x}-\frac{\partial\alpha}{\partial z}\right)+m\gamma'\left(\frac{\partial\alpha}{\partial y}-\frac{\partial\beta}{\partial x}\right) \\ =0 \end{aligned} \tag{A.20}$$

Like for the reflection, Hamilton establishes the integral

$$\rho + m\rho' = \text{const.} \tag{A.21}$$

"ρ, ρ' being the paths traversed by the light in going from any particular surface which cuts the incident rays perpendicularly, to the refractor (i.e.lens), and from the refractor to the focus."

Appendix B. The Hénon-Heiles Hamiltonian

Consider the Hénon-Heiles Hamiltonian

$$H = \frac{p_x^2 + p_y^2}{2} + \frac{x^2 + y^2}{2} - \frac{1}{3}(x^3 - 3xy^2)$$

The critical points are solutions of

$$\frac{\partial H}{\partial x} = x - x^3 + y^2 = 0 \qquad \frac{\partial H}{\partial y} = y + 2xy = 0 \qquad \frac{\partial H}{\partial p_x} = p_x = 0 \qquad \frac{\partial H}{\partial p_y} = p_y = 0$$

and are given by

$$x = y = 0 \qquad x = 1 \;\; y = 0 \qquad x = -\frac{1}{2} \;\; y = \frac{\sqrt{3}}{2} \qquad x = -\frac{1}{2} \;\; y = -\frac{\sqrt{3}}{2}$$

The first one is a minimum of V, the remainig three are saddles and are at the vertices of an equilateral triangle whose sides have length 1. The value of H at the saddle points is 1/6. Notice that we have

$$H - \frac{1}{6} = \frac{p_x^2 + p_y^2}{2} + \frac{1}{6}(1 + 2x)(3y^2 - (1 - x)^2) = 0$$

The stable region is given by $H \leq 1/6$. Notice that the intersection of $H = 1/6$ with the (x, y) plane is is $(1 + 2x)(3y^2 - (1 - x)^2) = 0$ and the stability region is the equilateral triangle defined by the intersection of the lines

$$x = -\frac{1}{2} \qquad\qquad y = \pm\frac{1}{\sqrt{3}}(1 - x)$$

whose vertices are the saddle points of H. We prove now that the the sphere of radius 1/2 defined by

$$x^2 + y^2 + p_x^2 + p_y^2 = \frac{1}{4}$$

is within the stability region defined by $H \leq 1/6$. To this end we introduce polar

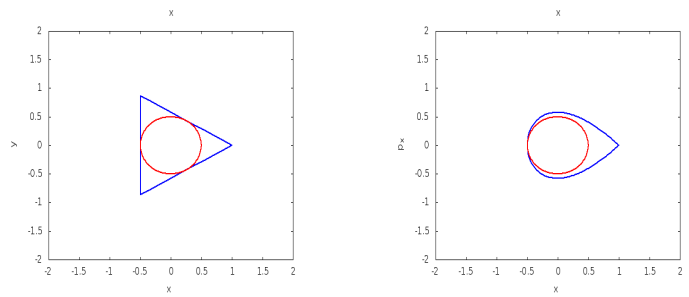

Fig. B1. Left panel: dynamic aperture blue line and bound (red line) in the (x, y) plane. Right panel: the same in the (x, p_x) plane

coordinates

$$x = r\cos\phi \qquad y = r\sin\phi \qquad\qquad p_x = p\cos\theta \qquad p_y = p\sin\theta$$

so that the Hamiltonian becomes

$$H = \frac{p^2}{2} + \frac{r^2}{2} + \frac{r^3}{3} f(\theta) \qquad f(\theta) = (3\cos\theta - 4\cos^3\theta)$$

Since $f(\theta)$ varies between -1 and 1 reaching the minimim at $\cos\theta = -1/2$, the maximum for $\cos\theta = 1/2$. As a consequence for fixed r and p we have

$$H \leq \frac{p^2}{2} + \frac{r^2}{2} + \frac{r^3}{3}$$

Notice that $r^2/2 + r^3/3 = 1/6$ for $r = 1/2$. Consider now the sphere of radius 1/2. For any point within the sphere $r^2 + p^2 \leq \frac{1}{4}$

$$H \leq \frac{p^2 + r^2}{2} + \frac{r^3}{3} \leq \frac{1}{8} + \frac{1}{3}\left(\frac{1}{4} - p^2\right)^{3/2} \leq \frac{1}{8} + \frac{1}{24} = \frac{1}{6}$$

As a consequence all the points of the sphere are within the stability domain. In figure 4 we show the dynamic aperture for the Hénon-Heiles Hamiltonian and the aperture disc of radius 1/2 in the x, y and x, p_x planes. In the x, p_x plane the boundary is

$$p_x = \pm\frac{1}{\sqrt{3}}(1 - x)\sqrt{1 + 2x}$$

References

1. W.R. Hamilton, Theory of systems of rays, *Transactions of Royal Irish Academy*, v. 15, (1828).
2. Jo. Bernoulli, Curvatura radii in diaphanis non uniformibus, Solutionque Problematis a se in Actis 1696 p. 269, propositi de invenienda Linea Brachystochrona [...], *Acta Eruditorum* (1697).
3. P. Freguglia, M. Giaquinta, The early period of the calculus of variations, Birkhauser-Springer, (2016).
4. R. Dugas,*A History of Mechenics*, Dover Publications inc. New York, (1988).
5. A. Bazzani, G. Servizi, E. Todesco, G. Turchetti, A normal form approach to the theory of nonlinear betatronic motion CERN-94-02, (1994).
6. A. Bazzani, A Hamiltonian approach to the non-linear geometrical optics, in Freguglia P., Turchetti G. ed. *Mechanics and Geometry*, Edizione Quattroventi, Urbino, pp.67-90,(2002).
7. A. Bazzani, P. Freguglia, L. Fronzoni, G. Turchetti An optical Hamiltonian experiment and beam dynamics, in *Nuclear Instruments & Methods in Physics Research*, Section A, **561**, pp.325-330, (2006).
8. L. Euler, Elementa calculi variationum, *Comm. Acad. Sci. Petropolitanae,* 10, (1764).
9. L. Euler, Methodus nova et facilis calculum variationum tractandi, *Comm. Acad. Sci. Petropolitanae*, 16 (1771).
10. M. Born, E. Wolf, *Principles of Optics*, Pergamon Press, Oxford, New York, (1970).
11. D. Holm and G. Kovacic, Homoclinic choas for ray optics in a fiber , *Physica D* **51**, p. 177 (1991).
12. G. Forte, F. Cecconi and A. Vulpiani, Transport and fluctuation-dissipation relations in asymptotiand preasymptotic diffusion across channels with variable section, *Phys. Rev E* **90**, p. 062110, (2014).
13. F. Cecconi, V. Blakaj, G. Gradoni and A. Vulpiani, Transport and fluctuation-dissipation relations in asymptotiand preasymptotic diffusion across channels with variable section, *Phys. Rev E submitted*, (2018).
14. E. Leonel, D. da Costa and C. Dettmann, Scaling invariance for the escape of particles from a periodically corrugated waveguide, *Physics Letters A* **376**, 421 (2012).
15. J. de Oliveira, C. Dettmann, D. , da Costa and E. Leonel, Scaling invariance of the diffusion coefficient in a family of two-dimensional Hamiltonian mappings,*Phys. Rev. E* **87**, p. 062904, (2013).
16. L.A.Bunimovich On the Ergodic Properties of Nowhere Dispersing Billiards, *Commun Math Phys.* **65 (3)**, 295312, (1979).
17. S. S. Abdullaev and G. M. Zavlaskii, Classical nonlinear dynamics and chaos of rays in problems of wave propagation in inhomogeneous media, *Usp. Fiz. Nauk.* **161**, p. 1 (1991).
18. D. Douglas, Chaotic billiard lasers , *Nature* **465**, p. 696 (2010).
19. S. Creagh, Directional Emission from Weakly Eccentric Resonators, *Phys. Rev. Lett.* **98**, p. 153901 (2007).
20. G. Tanner, Dynamical energy analysis Determining wave energy distributions in vibro-acoustical structures in the high-frequency regime, *Journal of Sound and Vibration* **98**, p. 153901 (2007).
21. G. Gradoni, J.-H. Yeh, B. Xiao, T. Antonsen, S. Anlage and O. E., Predicting the statistics of wave transport through chaotic cavities by the random coupling model: A review and recent progress, *Wave Motion* **51**, 606 (2014).